2005 RISP International Workshop on Nonlinear
Circuit and Signal Processing (NCSP'05)
Hawaii, USA, Mar. 4-6, 2005.

Research on Clutter Reduction Methods of a UWB Chaotic Radar

Natsumi Dake†, Yoko Uwate†, Yoshifumi Nishio† and Takaya Yamazato‡

† Dept. of Electrical and Electronic Eng., Tokushima University, Japan
Email: {dakera55, uwate, nishio}@ee.tokushima-u.ac.jp

‡ Center for Information Media Studies, Nagoya University, Japan
Email: yamazato@nuee.nagoya-u.ac.jp

1. Introduction

Chaos is nonperiodic and could generate sequences with infinite length theoretically. Although the sequences appear like noise, the values can be predicted exactly if the dynamics and the initial value are provided. If the feature of chaos is exploited well, some engineering systems with a new excellent performance could be invented.

On the other hand, a random noise radar using the UWB (Ultra Wide Band) technology has been proposed [1]. The motivation to use UWB stems from the need to have high range and velocity resolution, unambiguous range and velocity estimates, low probability of intercept, and immunity from interference. The random noise radar system transmits 1-2GHz UWB Gaussian random noise wave and the target is detected by a heterodyne correlation receiver. We have proposed a UWB chaotic radar [2] based on the random noise radar. The transmitted signal is replaced by a chaotic sequence generated by a simple chaotic map.

In this study, we focus mainly on removal of clutters by applying three clutter reduction methods. We apply the minimum distance approximation method, the maximum likelihood decoding method [3] and the affordable neural network method [4]. When we carried out computer simulations as changing the signal-to-noise ratio (S/N), probability distributions of recovered signals are shown.

2. UWB chaotic radar

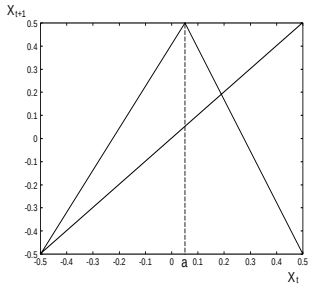

Figure 1: Skew tent map.

We use the skew tent map, which is known as the simplest chaos-generating map, to generate a chaotic sequence by OSC1. The skew tent map is shown in Fig. 1. We set the top coordinate of the skew tent map at $(a,\ 0.5)$, where a is a parameter having the range in $[-0.5,\ 0.5]$. The equation describing the skew tent map is as

$$x_{t+1} = \begin{cases} \dfrac{x_t}{0.5+a} + \left(0.5 - \dfrac{a}{0.5+a}\right) & (-0.5 \le x_t \le a) \\ \left(0.5 + \dfrac{a}{0.5-a}\right) - \dfrac{x_t}{0.5-a} & (a < x_t \le 0.5). \end{cases} \quad (1)$$

A block diagram of the UWB chaotic radar system is shown in Fig. 2. The detection is accomplished by a heterodyne correlation receiver.

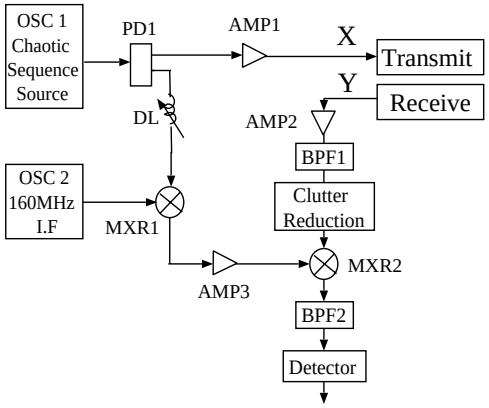

Figure 2: UWB chaotic radar.

At first, we give an initial value x_1 to the skew tent map with a constant parameter a. The generated chaotic sequence, which has a spectrum in 1-2GHz frequency range, passes through PD1 to duplicate signals. One is amplified and transmitted toward targets and the other is delayed and multiplied with the 160MHz sinusoidal signal generated by OSC2. The received echo signal Y including many clutters is expressed as follows;

$$Y = [y_1, y_2, \cdots, y_{N+1}] \quad (2)$$

$$y_t = x_t + \omega_t \qquad (1 \le t \le N+1). \quad (3)$$

where x_t is a generated chaos and ω_t is clutter. Clutter is an unnecessary reflection signals from the surface of the sea, the

rain, the cloud, and the obstacle such as buildings. In this simulation, AWGN (Additive White Gaussian Noise) is used to express all of the clutters.

In this study, we consider to remove clutters by using clutter reduction algorithms explained in the next section. The received echo signals Y are filtered and fed into a clutter reduction algorithm. At last, the output of clutter reduction is then multiplied with the delayed and up-converted chaotic signal and passes BPF having a center frequency of 160MHz and a bandwidth of 5MHz.

3. Clutter reduction methods

We consider three kinds of clutter reduction methods.

3.1. Minimum distance approximation method

At first, we consider a method using the minimum distance approximation. This method is the simplest noise cleaning method of chaotic signals. By using the two successive signals, the transmitted signal and the received signal (S/N 20dB) can be plotted on the 2-dimensional plane as Fig. 3.

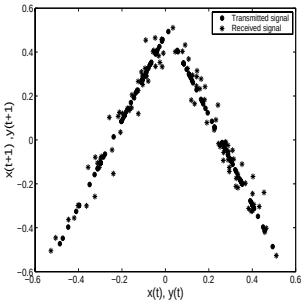

Figure 3: The transmitted signal and the received signal.

The transmitter signals should be on the skew tent map described by Eq. (1). However, the received signals are not on the map because of the clutters. This method is to modify the received signal into the point on the skew tent map which is the nearest to the received signal. The x-coordinate of the point can be calculated from the values of the received signals as follows;

$$v_t = \begin{cases} \dfrac{0.5+a}{a+(0.5+a)^2} \cdot \\ \left\{ y_{t+1} + y_t(0.5+a) - \left(0.5 - \dfrac{a}{0.5+a}\right) \right\} \\ \qquad (y_t \le a) \\ -\dfrac{(0.5-a)^2+1}{0.5-a} \cdot \\ \left\{ y_{t+1} - y_t(0.5-a) - \left(0.5 + \dfrac{a}{0.5-a}\right) \right\} \\ \qquad (y_t > a). \end{cases} \tag{4}$$

The output signal of this algorithm is given by V.

$$V = [v_1, v_2, \cdots, v_N]. \tag{5}$$

3.2. Maximum likelihood decoding method

Secondly, we consider a method using the maximum likelihood decoding. In this method, the skew tent map is divided into M states, and the dynamics is approximated by a Markov chain with transition probabilities corresponding to the mapping of each state.

The trellis diagram for the case of $M = 4$ is shown in Fig. 4.

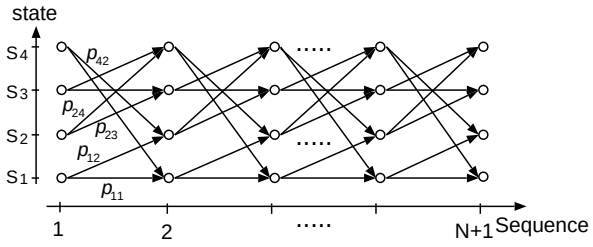

Figure 4: Trellis diagram (omit paths with probability=0).

where s_i is the quantized state and p_{ij} means the transition probability from the state i to the state j.

The maximum likelihood decoding algorithm carries out to find the best path in the trellis diagram.

1) Initialization : $t = 1$

$$\delta_1^j = |\hat{y_1} - s_j| \tag{6}$$

2) Forward pass : $2 \le t \le N+1$

$$\delta_t^j = \min_{1 \le i \le M} \left[\frac{\delta_{t-1}^i}{p_{ij}} \right] |\hat{y_t} - s_j|, \qquad \phi_t^j = \arg[\delta_t^j] \tag{7}$$

3) Termination : $t = N+1$

$$w_N = \arg \left[\min_{1 \le j \le M} [\delta_N^j] \right] \tag{8}$$

4) Backward pass

$$w_t = \phi_{t+1}^{w_{t+1}} \qquad t = N-1, N-2, \cdots, 1. \tag{9}$$

This algorithm computes the hamming distance of each state and the quantized received signal $\hat{y}_t$. We calculate δ_t^j and preserve a minimum value in ϕ_t^j by the forward pass. And the minimum value is chosen by the termination $t = N+1$, the operation is executed by the backward pass. As a result, the best pass W can be chosen.

$$W = [w_1, w_2, \cdots, w_N]. \tag{10}$$

3.3. Affordable neural network method

We consider a method using the affordable neural network, which has been proposed by the authors recently. The affordable neural network is one of feedforward neural network that applies the back propagation learning. Some extra neurons in the hidden layer are prepared in advance. For learning process, all of the neurons in the hidden layer are not used, and

operating neurons in the hidden layer changes at every updating.

By giving a certain amount of chaotic sequences obtained from the skew tent map as teacher signals, we train the network to output chaotic sequences generated by only the skew tent map. After the learning, we input the received signal into the network. If the learning of the network can be achieved completely, the clutter in the received signals should be removed. The output of the network is given by Z.

$$Z = [z_1, z_2, \cdots, z_N]. \tag{11}$$

4. Simulation result

In the following computer simulations, the parameter of the skew tent map is fixed as $a = 0.01$, and the chaotic sequence length is fixed as $N = 50$. The target detections using the three methods are carried out.

(1) The minimum distance approximation method $(Method\ 1)$,
(2) The maximum likelihood decoding method $(Method\ 2)$,
(3) The affordable neural network method $(Method\ 3)$.

For comparison,
(4) Without any clutter reduction methods $(No\ Reduction)$ is also carried out.

At first, we carried out computer simulations for the case of $No\ Reduction$. The probability distribution of power after passing BPF2 is shown in Fig. 5, when 10,000 chaotic sequences with different initial values are transmitted. The horizontal axis is the power and the vertical axis is probability. The left graph shows the result for the case that the received signal is only clutters. While the right graph shows the result for the ideal case of no clutters. From the figure, we can say that the detection probability of a target is 100% if the threshold is set between 13 and 18.

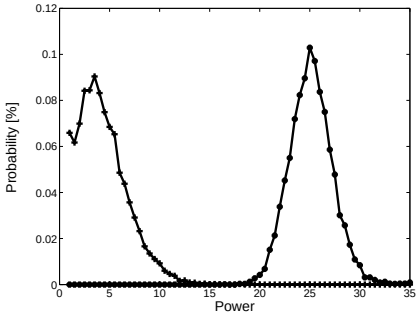

Figure 5: Probability distribution of $Power$.

Next, we carried out computer simulations as changing S/N from 5dB to 20dB. Figure 6 shows the probability distributions after passing BPF2. For $Method\ 2$, the quantization of the skew tent map is $M = 64$. For $Method\ 3$, the number of learning pattern is set to 1000. Further, the parameter of the inertia rate is fixed as $\eta = 0.02$ and initial values of the weights are given between -1.0 and 1.0 at random. The learning time is set to 50,000. We prepare 50 neurons in input layer, 100 neurons in hidden layer, and the number of affordable neurons is set to 10. From Figs. 6(a), (b) and (c), we can say that the distributions of all three methods shift to the right compared with the result of $No\ Reduction$. This means that the wrong warning probability decreases and the detection probability increases. From Fig. 6(d), for 20dB, the four distributions are almost same. This is why the received signals are almost the same as the transmitted signal.

In order to confirm the clutter removal ability of the three methods, the distances between the transmitted signals and the recovered signals are calculated. The results are shown in Fig. 7. Figure 7(a) and (b) show the results for small S/N and for large S/N, respectively. The distance are calculated by the following equations;

$$\begin{aligned} D_1 &= \sum_{t=1}^{N}(v_t - x_t)^2, \quad D_2 = \sum_{t=1}^{N}(w_t - x_t)^2, \\ D_3 &= \sum_{t=1}^{N}(z_t - x_t)^2, \quad D_{No} = \sum_{t=1}^{N}(y_t - x_t)^2. \end{aligned} \tag{12}$$

From Fig. 7(a), for small S/N, the $Method\ 2$ achieves the best performance to remove clutters. The performance of the $Method\ 1$ is worse than the $Method\ 2$. This is because $Method\ 1$ uses only two values in each removing process. However, the $Method\ 1$ is very simple, computational cost is small even for long N. The performance of the $Method\ 3$ is not very good. However, it is difficult to find a good parameter set of the $Method\ 3$. We still believe that the well-tuned $Method\ 3$ could remove the clutters effectively.

From Fig. 7(b), for large S/N, the $Method\ 1$ achieves the best performance to remove clutters. On the other hand, the performance of the $Method\ 2$ does not become less than around 0.05. This is because $Method\ 2$ includes unavoidable quantization errors.

Finally, we investigated the detection probability when the three clutter reduction methods are applied by computer simulations as changing S/N. The threshold of the probability of $Power$ is set 20 and 25. From the results, we can say that all three reduction methods contribute to increase the detection probability as shown in Fig. 8, especially for smaller S/N.

5. Conclusions

In this study, the three clutter reduction methods have been applied to the chaotic UWB radar. The basic properties of the methods have been investigated by computer simulations.

References

[1] M. Dawood, Ram R. Narayanan, "Receiver operating characteristics for the coherent UWB random noise radar," IEEE Trans. Aerospace Electronic Syst., vol. 37, no. 2, pp. 586-594, 2001.
[2] N. Dake, Y. Nishio, T. Yamazato, "UWB radar system using chaotic signal," Proc. IEICE General Conference, no. SA-2-6, pp. S11-S12, 2004.
[3] A. Kisel, H. Dedieu, T. Schimming, "Maximum Likelihood Approaches for Noncoherent Communications with Chaotic Carriers," IEEE Trans. Circuits and Syst., vol. 48, no. 5, pp. 533-542, 2001.
[4] Y. Uwate, N. Dake, Y. Nishio, "Back propagation Learning of an Affordable Neural Network for Chaotic Time Series," Proc. NCSP'05, 2005 (to appear).

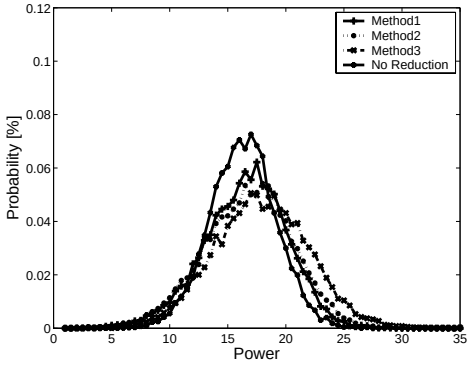

(a) 5dB.

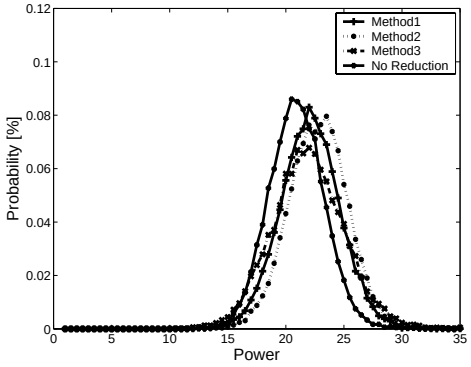

(b) 10dB.

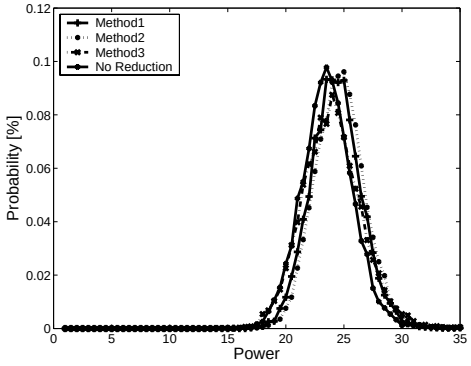

(c) 15dB.

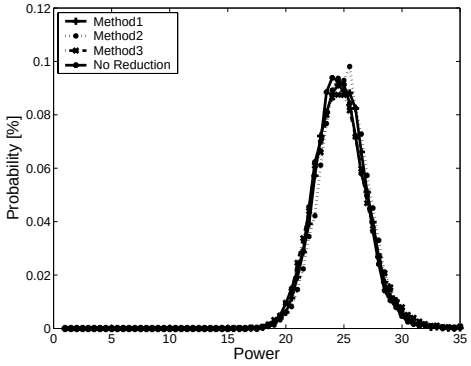

(d) 20dB.

Figure 6: Probability distribution of $Power$.

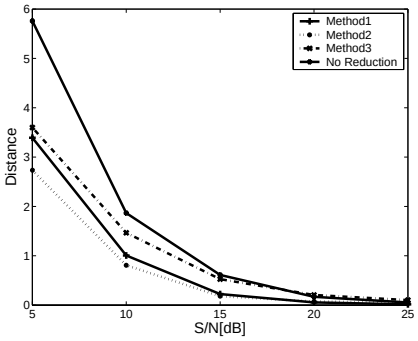

(a)

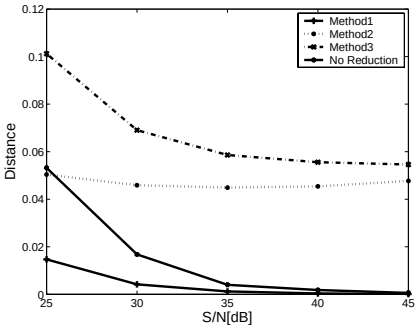

(b)

Figure 7: Distance between the transmitted signals and the recovered signals.

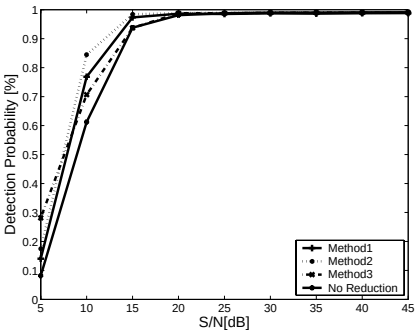

(a) Threshold: 20.

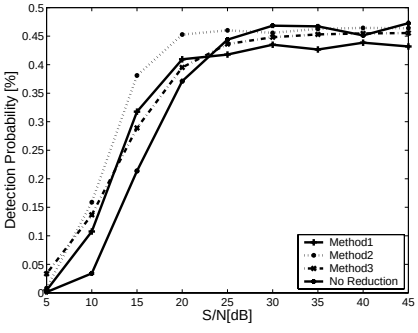

(b) Threshold: 25.

Figure 8: Detection Probability.